Ninth International Conference on
THIN-WALLED STRUCTURES – ICTWS2023
Sydney, Australia, Nov 29 – Dec 1, 2023

LATERAL-TORSIONAL BUCKLING RESISTANCE OF NON-UNIFORM MONO-SYMMETRIC STEEL BEAMS

Luís Simões da Silva*, José O. Gomes Jr*, T. Tankova, H. Carvalho*** and José O. F. Filho***

* University of Coimbra
e-mails: luisss@dec.uc.pt, jose.junyor@student.dec.uc.pt, jose.filho@dec.uc.pt

** Delft University of Technology
e-mail: t.tankova@tudelft.nl

*** Federal University of Minas Gerais
e-mail: hermes@dees.ufmg.br

Keywords: Stability; Steel; Eurocode 3; General formulation; Mono-symmetric beams.

Abstract. *The lateral-torsional resistance of prismatic double-symmetric I-section beams is accurately predicted using a mechanically consistent Ayrton-Perry approach, combined with a calibrated generalized imperfection. The corresponding design formulation was recently adopted in the revised version of Eurocode 3. However, for mono-symmetric I-sections, Eurocode 3 enforced the use of the General case that highly underestimates the lateral-torsional buckling resistance of doubly symmetric beams and shows a large scatter of results. In case of non-uniform beams with generic boundary conditions or loading, a General Formulation was recently proposed and shown to yield good results for doubly symmetric cross sections. This paper presents an extension of the General Formulation to mono-symmetric cross-sections. The methodology was validated against experimental results and a large parametric study using advanced FEM simulations. The results show significant improvements when compared to the General Case, with low scatter and on the safe side.*

1 INTRODUCTION

Tapered steel beams with thin-walled welded I-sections are commonly used due to their efficiency in bending and ease of fabrication. The use of monosymmetric cross-sections further increases their efficiency, mainly when the area of the flange under compression is increased, being widely used in crane girders, pitched-roof portal frames and often as part of composite girders in bridge decks.

The effect of monosymmetry on the lateral-torsional buckling behavior of I-section beams has been investigated by many researchers, mostly focused on the elastic critical buckling moment [1-12] that resulted in several tables, charts, and approximate expressions. Concerning the nonlinear behaviour of monosymmetric beams it was shown that the lateral buckling resistance depends not only on the pre-buckling deformation, but also on section shape, load distribution, and if the largest flange is under compression or tension [13-16]. Recently, experimental tests and numerical simulations [17-20] addressed the study of the ultimate resistance of monosymmetric I-section beams made with high strength steels, evaluating the influence of initial geometric imperfections and residual stresses, to improve the current design rules.

The behavior of tapered monosymmetric I-beams was also examined in the literature [21-26], in which numerical models and formulations were developed to analyze the lateral-torsional buckling behavior of such elements. Marques et al. [27] calibrated a generalized imperfection for web-tapered beams in the scope of the buckling curve approach with an

extensive numerical parametric study that was verified with recent experimental tests on tapered beams [28, 29] yielding excellent results. Finally, more recently, Tankova et al. [30, 31] developed a design-oriented general formulation for the stability design of steel columns, beams, and beam-columns with variable geometry, loads and different support conditions that was also extensively validated for tapered beams.

Currently, in part 1-1 of Eurocode 3 (EC3-1-1) [32], the lateral-torsional buckling resistance of monosymmetric beams is assessed using the General Case (GC) or, for non-prismatic beams, the General Method (GM). For doubly-symmetric beams, the GC provides very conservative results with large scatter [33] and the GM, besides being empirical leads to similar results as the GC for prismatic beams [34]. This paper presents an extension of the General Formulation [30] to mono-symmetric cross-section beams with arbitrary variation of the cross-section or bracings along the length of the beam.

2 GENERAL FORMULATION FOR MONO-SYMMETRIC BEAMS

The utilization ratio of a generic single member may be expressed by equating the total longitudinal stress, σ, due to first and second order forces, to the yield stress, f_y:

$$\frac{\sigma(x)}{f_y} = \frac{N(x)}{A(x)f_y} + \frac{M_y(x)}{W_y(x)f_y} + \frac{M_z(x)}{W_z(x)f_y} + \frac{M_y^{II}(x)}{W_y(x)f_y} + \frac{M_z^{II}(x)}{W_z(x)f_y} + \frac{M_w^{II}(x)}{W_w(x)f_y} \tag{1}$$

where $A(x)$ is the cross-section area, $W_y(x)$ and $W_z(x)$ are the section moduli relative to the y- and z-axes, respectively, and $W_w(x)$ is the warping modulus at location x along the member. It is noted that for section classes 1 and 2 the plastic section moduli should be used. Then, as long as the second order contributions can be determined, the buckling resistance may be verified for an appropriate number of locations along the member, as follows:

$$\frac{N(x)}{A(x)f_y} + \frac{M_y(x)}{W_y(x)f_y} + \frac{M_z(x)}{W_z(x)f_y} + \frac{M_y^{II}(x)}{W_y(x)f_y} + \frac{M_z^{II}(x)}{W_z(x)f_y} + \frac{M_w^{II}(x)}{W_w(x)f_y} \leq 1.0 \tag{2}$$

The verification of a single member with variable geometry, boundary conditions, subject to arbitrary loading, is done by verifying Eq. (2) at enough locations along the member. At each position, the respective values of the first order axial force, $N(x)$, bending moments $M_y(x)$, $M_z(x)$, second order contributions obtained from the relevant buckling mode and cross-section properties, $A(x)$, $I_z(x)$, etc. are to be used. For prismatic members, all these buckling cases are covered by EC3-1-1 [32] design rules. The only condition is that the designer needs to choose is the relevant buckling mode and the corresponding verification format.

For lateral-torsional buckling of mono-symmetric beams, the general interaction Eq. (2) becomes:

$$\frac{\sigma(x)}{f_y} = \frac{M_y(x)}{W_y(x)f_y} + \frac{M_z^{II}(x)}{W_z(x)f_y} + \frac{M_w^{II}(x)}{W_w(x)f_y} \tag{3}$$

where there are two second-order contributions, the out-of-plane bending moment depending on the lateral displacement:

$$M_z^{II}(x) = -EI_z(x)v"(x) \tag{4}$$

and the bi-moment depending on the twist rotation:

$$M_w^{II}(x) = -EI_w(x)\left(\theta"(x) + \frac{2}{h}\theta'(x)h'\right) \tag{5}$$

Hence, when considering the amplitude of the initial imperfection both components (lateral displacement and twist rotation) must be considered. For simply supported beams it is possible to obtain the amplitude by the coupling of the lateral displacement and twist rotation [35]. In a more general configuration (variation of the geometry along the member, different boundary and loading conditions, etc.), this relationship may not be held. For that reason, it was chosen to use both components of the mode shape as initial imperfection, assuming that they are multiplied by the same amplitude:

$$v_0(x) = v_{cr}(x)\bar{\delta}_{0,LTB} \qquad \theta_0(x) = \theta_{cr}(x)\bar{\delta}_{0,LTB} \tag{6}$$

The resulting amplification relationship for the displacement and rotation is given by:

$$v(x) = \frac{1}{\alpha_{cr}-1} v_0(x) \qquad \theta(x) = \frac{1}{\alpha_{cr}-1} \theta_0(x) \tag{7}$$

It is assumed that the real beam should have the same resistance as an equivalent beam with fork supports and constant bending moment. This equivalent beam has the same geometry as the real beam at the critical cross-section and the same elastic critical moment. Hence, it is possible to obtain the required generalized imperfection by setting equal the second order utilization for the equivalent and real beams. The second order moments for a simply supported beam at mid-span are given by:

$$M_z^{II}(x_m) = M_{y,Ed}\theta_{tot} = M_{y,Ed}\theta_0 \frac{1}{1-1/\alpha_{cr}} = \frac{\alpha_{cr} M_{y,Ed}(x_m)\bar{e}_0\theta_{cr}(x_m)}{\alpha_{cr}-1} \tag{8}$$

$$\begin{gathered} M_w^{II}(x_m) = M_{y,Ed}v_{tot} - GI_t\theta - M_{y,Ed}\beta\theta_{tot} = \\ = M_{y,Ed}v_0 \frac{1}{1-1/\alpha_{cr}} - GI_t\left(\theta_0 \frac{1}{1-1/\alpha_{cr}} - \theta_0\right) - M_{y,Ed}\beta\theta_0 \frac{1}{1-1/\alpha_{cr}} = \\ = \frac{\alpha_{cr} M_{y,Ed}(x_m)\bar{e}_0\theta_{cr}(x_m)}{\alpha_{cr}-1}\left(\frac{v_0(x_m)}{\theta_0(x_m)} - \frac{GI_t(x_m)}{M_{cr}} - \beta(x_m)\right) \end{gathered} \tag{9}$$

where $\beta(x)$ is a factor that incorporates the Wagner effect [36] due to the mono-symmetry. The second order utilization ratio for the equivalent member is given by:

$$\begin{gathered} \varepsilon_M^{II}(x_m) = \frac{M_z^{II}(x_m)}{W_z(x_m)f_y} + \frac{M_w^{II}(x_m)}{W_w(x_m)f_y} = \\ = \frac{\alpha_{cr} M_{y,Ed}(x_m)\bar{e}_0\theta_{cr}(x_m)}{W_z(x_m)f_y(\alpha_{cr}-1)}\left(1 + \frac{v_{cr}(x_m)}{\theta_{cr}(x_m)}\frac{W_z(x_m)}{W_w(x_m)} + \frac{GI_t(x_m)}{M_{cr}}\frac{W_z(x_m)}{W_w(x_m)} + \beta(x_m)\frac{W_z(x_m)}{W_w(x_m)}\right) = \\ = \frac{N_{cr,z}\bar{e}_0}{W_z(x_m)f_y(\alpha_{cr}-1)} \end{gathered} \tag{10}$$

with

$$N_{cr,z} = \alpha_{cr} M_{y,Ed}(x_m)\theta_{cr}(x_m)\frac{W_z(x_m)}{W_w(x_m)}\left(\frac{W_w(x_m)}{W_z(x_m)} + \frac{v_{cr}(x_m)}{\theta_{cr}(x_m)} + \frac{GI_t(x_m)}{M_{cr}} + \beta(x_m)\right) \tag{11}$$

The second order utilization of the real beam at the location x_m is given by:

$$\begin{gathered} \varepsilon_M^{II}(x_m) = \frac{M_z^{II}(x_m)}{W_z(x_m)f_y} + \frac{M_w^{II}(x_m)}{W_w(x_m)f_y} = \\ = \frac{EI_z(x_m)}{W_z(x_m)f_y(\alpha_{cr}-1)}\left[v''_{cr}(x_m) + \frac{W_z(x_m)}{W_w(x_m)}\frac{I_w(x_m)}{I_z(x_m)}\left(\theta''_{cr}(x_m) + \frac{2}{h}\theta'_{cr}(x_m)h'\right)\right]\bar{\delta}_0 \end{gathered} \tag{12}$$

Equalling the second order utilization ratio for the equivalent beam and the real beam at the location x_m leads to the following expression for the amplitude of the imperfection:

$$\bar{\delta}_{0,LTB} = \frac{N_{cr,z}\bar{e}_0}{EI_z(x_m)\left[v''_{cr}(x_m)+\frac{W_z(x_m)\,I_w(x_m)}{W_w(x_m)\,I_z(x_m)}\left(\theta''_{cr}(x_m)+\left(\frac{2}{h}h'\right)\theta_{cr}'(x_m)\right)\right]} = f_\eta \bar{e}_0 \tag{13}$$

This amplitude is used with the proposed generalization. It contains the equivalent geometrical imperfection $\bar{e}_0$ but also additional terms ensuring consistency with the Eurocode 3 design rules. Ideally, x_m should be chosen as the correct critical location. In order to avoid an iterative procedure, the location x_m is adopted where $v''_{cr}(x)$ reaches a maximum. The amplitude of the generalized imperfection is given by:

$$\eta^*(x) = \alpha\left(\bar{\lambda}(x) - 0.2\right) f_\eta \left|\delta^{fl}(x)\right| \frac{W_z(x)}{A(x)} \tag{14}$$

$$f_\eta = \frac{N_{cr,z}}{EI_z(x_m)\left[v''_{cr}(x_m)+\frac{W_z(x_m)\,I_w(x_m)}{W_w(x_m)\,I_z(x_m)}\left(\theta''_{cr}(x_m)+\left(\frac{2}{h}h'\right)\theta_{cr}'(x_m)\right)\right]} \tag{15}$$

For monosymmetric I-sections, the general displacement of the critical mode, $\delta^{fl}(x)$, is given by a geometric relationship between the lateral displacement and the section rotation, as defined by Eq. (16) and Figure 1:

$$\delta^{fl}(x) = v_{cr}(x) + \left(h(x) - z_G(x) + z_0(x)\right)\theta_{cr}(x) \tag{16}$$

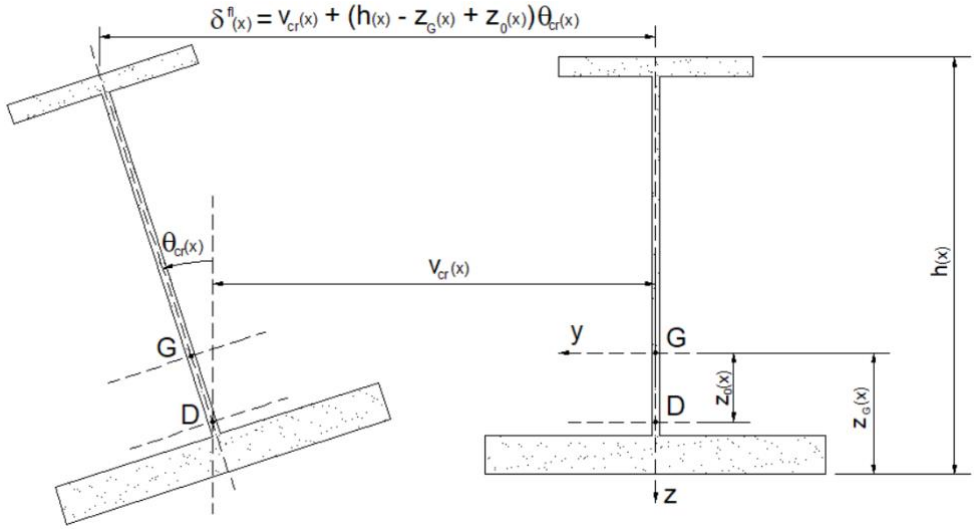

Figure 1: General displacement of the critical mode for mono-symmetric I-sections.

Thus, the final verification equation is given by:

$$\varepsilon_M(x) = \frac{M_{y,Ed}(x)}{W_y(x) f_y} + \frac{EI_z(x)\left[v''_{cr}(x)+\frac{W_z(x)\,I_w(x)}{W_w(x)\,I_z(x)}\left(\theta''_{cr}(x)+\left(\frac{2}{h}h'\right)\theta_{cr}'(x)\right)\right]}{A(x) f_y(\alpha_{cr}-1)}\,\eta(x) \le 1.0 \tag{17}$$

with

$$\eta(x) = \alpha\left(\bar{\lambda}(x) - 0.2\right) f_\eta \left|\delta^{fl}(x)\right| \tag{18}$$

An equivalent elastic critical force $N_{cr,z,eq}$ is "retrieved" from the buckling mode using the differential equation for flexural buckling:

$$EI_z(x)v''_{cr}(x) - N_{cr,z}v_{cr}(x) - z_0 N_{cr,z}\theta_{cr}(x) = 0. \quad (19)$$

Then, the equivalent force becomes:

$$N_{cr,z,eq} = \frac{EI_z(x_m)|v''_{cr}(x_m)|}{|v_{cr}(x_m)+z_0\theta_{cr}(x)|} \quad (20)$$

It is this force that is used for the calculation of the normalized slenderness:

$$\bar{\lambda}(x) = \sqrt{\frac{A(x)f_y}{N_{cr,z,eq}}}. \quad (21)$$

3 NUMERICAL MODELLING

3.1 Description of the numerical model

The numerical analyses were performed using the finite element software Ansys (version 22.0) [37]. The geometry of the models was implemented according to the nominal dimensions of the sections. The SHELL181 element, which is composed by 4 nodes with 6 degrees of freedom per node, was chosen to discretize the mesh. After a mesh sensitive study, 16 elements were defined across the flange´s width and 16 across the web´s depth (see Figure 2). The same size of the elements across the width and depth was used along the length of the member, generating only quadrangular elements (see Figure 2).

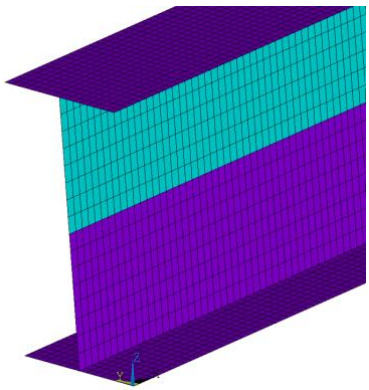

Figure 2: Representation of the mesh for an I-section member.

Geometrically and materially nonlinear analyses with imperfections (GMNIA) were executed to obtain the ultimate resistance of the numerical models by using the arc-length method and the von Mises failure criterion. Initial geometric imperfections were introduced with the shape corresponding to the first global buckling mode obtained from a previous linear buckling analysis (LBA). The validation models were run considering the material stress-strains curve, residual stress diagram and amplitude of geometrical initial imperfections obtained by experimental tests found in the literature. In the parametric study, following ECCS [38] recommendations, an amplitude of imperfection equal to $L/1000$ and a pattern of welded residual stresses is implemented in the numerical models. The constitutive law adopted for the parametric study follows prEN 1993-1-14 [39] for hot-rolled steels with a yield plateau and strain hardening.

3.2 Numerical Model Validation

The numerical model is validated with the experimental results from Tankova et al. [17] and Lebastard [29]. The experimental model of Tankova et al. [17] is a four-point bending model

where vertical forces are applied in two locations, as shown in Figure 3. Fork-support conditions are considered at the extremities, where additional lateral supports are considered at the location of vertical forces application (see Figure 3). All prototypes are 6 m long, with an unbraced distance between the vertical forces equal to 4 m. The main parameters of the mono symmetric I section are shown in Table 1.

Figure 3: Numerical Models based on experimental prototypes geometry of Tankova et al. [17].

Table 1: Experimental parameters from Tankova et al. [17] used in the numerical model validation.

Prototype	Member	$\bar{\lambda}_{LT}$	Fab.	Steel grade		Section classification	Geometrical Imperfections (mm)*	
				Flanges	Web		In-plane	Out-of-plane
B11	700 X 200(400) X 8 X 16	1.01	Welded	S690	S690	4	0.96	0.34
B12		1.00		S690	S355		0.07	4.48
B13		0.84		S460	S460		1.31	0.90
B14		0.83		S460	S355		1.93	1.29

* Measurements at mid-span.

Table 2 and Figure 4 compare the experimental and the numerical results for the ultimate load strength (P_{ult}) for the geometries exhibited in Table 1. There is excellent agreement between the numerical and experimental results, in terms of rigidity and ultimate load capacity. All numerical models, as well the experimental ones, failed by lateral-torsional buckling.

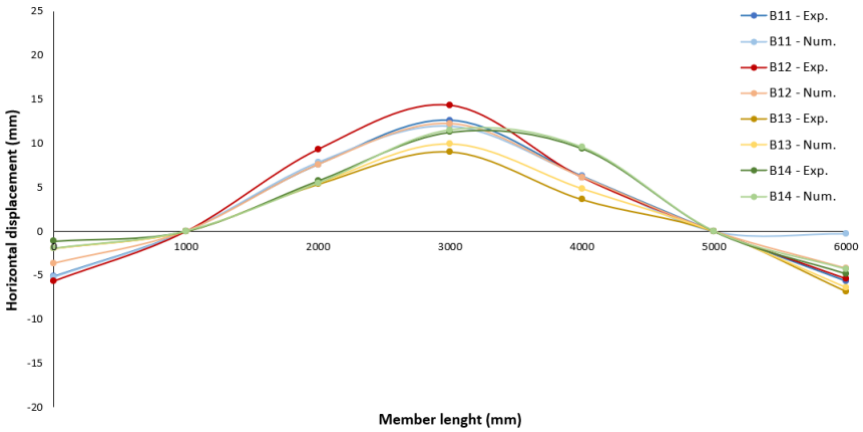

Figure 4: Horizontal displacements at maximum load – displacements measured at the middle of the web.

Table 2: Experimental and numerical results for P_{ult}, considering the experimental results from Tankova et al. [17].

Prototype	P_{ult} (kN)		Num./Exp.
	Experimental	Numerical	
B11	1731.80	1731.96	1.00
B12	1601.03	1610.89	1.01
B13	1307.18	1301.13	1.00
B14	1133.28	1210.02	1.07

Additionally, the numerical model is validated against the experimental results from Lebastard [29]. This experimental program includes lateral torsional buckling tests on two uniform and two tapered members, one having a mono-symmetric cross-section while the other is doubly symmetrical within both groups. Table 3 compares the experimental and numerical results for the ultimate load of these beams, showing good agreement between the numerical and the experimental results.

Table 3: Experimental and numerical results for P_{ult}, considering the experimental results from Lebastard [29]

	P_{ult} (kN)		
Prototype	Experimental	Numerical	Num./Exp.
U-DS	747.60	733.60	0.98
U-MS	903.60	887.31	0.98
T-DS	720.60	684.63	0.95
T-MS	775.80	726.31	0.94

3.3 Parametric Study

To assess the general formulation for mono-symmetric I-section (see Section 2), the following parametric study was considered, divided into two subsets as follows:

- prismatic beams subjected to linear bending moment, distributed load and point load, with fork boundary conditions - see Table 4 –, totaling 492 numerical models;

Table 4: Parametric study for prismatic mono-symmetric cross-sections.

Section $h\ x\ b_2(b_1)\ x\ t_w\ x\ t_2(t_1)$	L (m)	Steel grade	Bending Moment diagram	Stress on the largest flange
300 x 150(150) x 8 x 20(15) 300 x 150(150) x 8 x 30(20) 400 x 180(180) x 10 x 30(20) 400 x 180(180) x 10 x 40(25) 500 x 200(150) x 12 x 50(30)	4 6 8 10	S235 S355 S460	Linear (ψ = 1.0, 0.0 and -1.0)	Tension Compression
400 x 180(180) x 10 x 40(25) 500 x 200(150) x 12 x 50(30) 430 x 350(200) x 8 x 40(20)			Distributed load (applied at the top face - TF, the centroid - G, the torsion center - D and the bottom face - BF)	Tension
400 x 180(180) x 10 x 40(25)			Point load (applied at the top face -TF, the centroid - G, the torsion center - D and the bottom face - BF)	

- tapered beam h x 300(200) x 8 x 16(16), with the largest and the smallest depth equal to 500 and 250, respectively; 12 m-length ($\bar{\lambda}_z$ = 1.30); S235 grade steel; largest flange in tension; subjected to distributed load (TF, BF, G and D point loading application); clamped boundary conditions at the end extremity with the largest depth and for boundary conditions at the other end; only the smallest flange is inclined. Additionally, three cases were studied: member with restraint at the flange in tension, located at (i) mid-span and (ii) at 1/3 and 2/3 of the length; (iii) and member with restraint at the flange in compression, located at mid-span. Number of numerical models: 18.

4 VALIDATION OF THE GENERAL FORMULATION FOR MONO-SYMMETRIC BEAMS

4.1 Prismatic mono-symmetric cross sections

Figure 5 presents the scatter plot of r_t x r_e for the different loading types for the prismatic mono-symmetric cross sections subset, where r_e is the ratio between the numerical lateral-torsional buckling resistance and the plastic bending moment resistance of the cross section,

and r_t is the ratio between the analytical buckling resistance (EC3-General Case or General Formulation) and the cross-sectional plastic bending moment resistance. In general, both approaches provide safe-sided results. However, EC3-General Case (GC) rules are too conservative for all cases studied, while the General Formulation (GF) yields more accurate estimates of the lateral-torsional buckling resistance. The statistical evaluation of the GC and GF (see Table 5) are carried out based on the ratio (r_N) between the numerical lateral-torsional buckling resistance and the analytical lateral-torsional buckling resistance, leading to an average $r_N = 1.49$ and a c.o.v of 5.7% for the GC and an average $r_N = 1.13$ and a c.o.v of 2.4% for the GF.

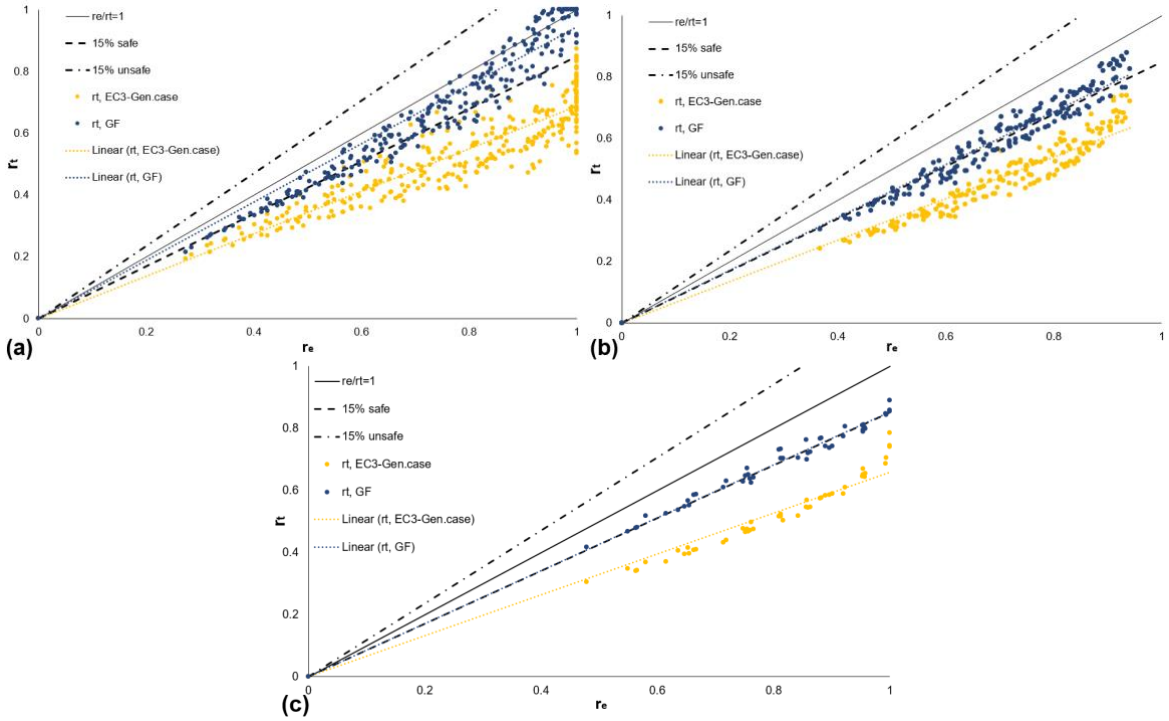

Figure 5: Scatter plot: (a) linear bending moment, (b) distributed load, (c) point load.

Table 5: Statistical Parameters for linear bending moment distribution.

Subset	n	$r_{N,EC3-General\ Case}$					$r_{N,General\ Formulation}$				
		Average	St.Dev.	Cov	Min	Max	**Average**	St.Dev.	Cov	Min	Max
LBM	300	**1.47**	0.10	6.59	1.36	1.58	**1.09**	0.02	1.93	1.07	1.12
UDL	144	**1.52**	0.06	4.02	1.47	1.59	**1.19**	0.04	3.51	1.14	1.24
CL	48	**1.55**	0.09	5.60	1.27	1.66	**1.17**	0.03	2.56	1.11	1.22
ALL	492	**1.49**	0.09	5.74	1.27	1.66	**1.13**	0.03	2.45	1.07	1.24

4.2 Tapered mono-symmetric cross sections

Figure 6 shows the scatter plot r_t x r_e for the monosymmetric tapered beams and Table 6 exhibits the comparison between the numerical lateral-torsional buckling resistance and the corresponding analytical results according to the General Method (GM) and the proposed extension of the General Formulation (GF), in terms of the r_N ratio. The GM shows poor results that are unacceptably conservative, with an average $r_N = 2.12$ and a c.o.v of 9.1%. The results of GF are considerably closer to the numerical values, leading to an average $r_N = 1.14$ and a c.o.v of 3.3%, exhibiting a similar performance when compared to the prismatic cases.

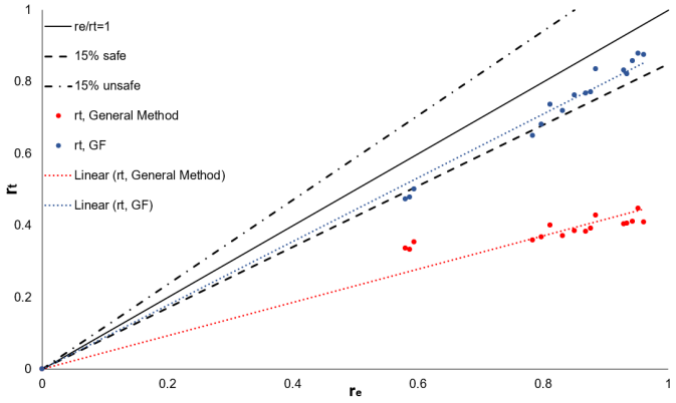

Figure 6: Scatter plot for the mono-symmetric tapered members.

Table 6: Comparison between General Method and the General Formulation.

Case	$r_{N,General\ Method}$	c.o.v. (%)	$r_{N,General\ Formulation}$	c.o.v. (%)
No Restraints	2.09	11.9	1.18	3.3
1 restraint at flange in tension	2.13	11.7	1.17	3.9
2 restraints at flange in tension	1.97	10.1	1.11	5.2
1 restraint at flange in compression	2.29	2.5	1.11	0.9
ALL	**2.12**	9.1	**1.14**	3.3

5 CONCLUSIONS

The General Formulation proposed by Tankova et al. [30] was extended for mono-symmetric beams with variable geometry, boundary conditions, subject to arbitrary loading. A calibrated advanced FEM numerical model was used to carry out a large parametric study on prismatic and tapered beams, leading to the following conclusions:

- The application of the General Case and the General Method as specified in EC3-1-1 lead to very conservative results.
- The extended General Formulation leads to good and consistent results. For non-prismatic beams with several bracing conditions, the results of the General Method are very poor, while the General Formulation maintains the good consistency with the prismatic cases.
- The General Formulation is easily incorporated in structural design software or as a standalone excel sheet verification because its practical implementation consists of a sequence of cross-sectional checks.

REFERENCES

[1] Kitpornchai S. and Trahair N.S., "Buckling Properties of Monosymmetric I-Beams", *Proceedings ASCE, Journal of the Structural Division*, **106**(5), 1980.

[2] Roberts T.M. and Burt C.A., "Instability of Monossymetric I-Beams and Cantilevers", *Int. J. Mech. Sci.*, **27**(5), 313-324, 1985.

[3] Roberts T.M. and Azizian Z.G., "Influence of pre-buckling displacements on the elastic critical loads of thin walled bars of open cross-section", *Int. J. Mech. Sci.*, **25**, 93-104, 1983.

[4] Roberts T.M., "Second-order strains and instability of thin-walled bars of open cross-section", *Int. J. Mech. Sci.*, **23**, 297-306, 1981.

[5] Wang C.M. and Kitipornchai S., "On stability of monosymmetric cantilevers", *Eng. Struct.*, **8**(3), 169-80, 1986.

[6] Wang C.M., Kitipornchai S. and Thevendran V., "Buckling of braced monosymmetric cantilevers". *Int J Mech Sci.*, **29**(5), 321-37, 1987.

[7] Vlasov V.Z., *Thin-walled elastic beams (Moscow 1940) (2nd edn)*. Israel Program for Scientific Translations, Jerusalem, 1961.

[8] Goodier J.N., *Flexural-torsional buckling of bars of open section under bending, eccentric thrust or torsional loads. Bulletin 28,* Cornell University Engineering Experimental Station, 1942.

[9] Anderson J.M. and Trahair N.S., "Stability of monosymmetric beams and cantilevers", *Proceedings ASCE, Journal of the Structural Division*, **98**, 269-286, 1972.

[10] Clark J.W. and Hill H.N., "Lateral Buckling of Beams". *Proceedings ASCE, Journal of the Structural Division*, **68**, ST7, 1960.

[11] Andrade A., Camotim D., Providência e Costa P., "On the evaluation of elastic critical moments in doubly and singly symetric I-section cantilevers", *Journal of Constructional Steel Research,* **63**, 894-908, 2007.

[12] Camotim D., Andrade A. and Basaglia C., "Some thoughts on a surprising result concerning the lateral-torsional buckling of monosymmetric I-section beams", *Thin-Walled Structures,* **60**, 216-221, 2012.

[13] Nethercot D.A., "Inelastic buckling of monosymmetric I-beams", *Proceedings ASCE, Journal of the Structural Division*, **99**(ST7), 1696-1701, 1973.

[14] Mohri F., Damil N. and Potier-Ferry M., "Linear and non-linear stability analyses of thin-walled beams wit monosymmetric I sections", *Thin-Walled Structures*, **48**, 299-315, 2010.

[15] Trahair N.S., "Inelastic buckling design of monosymmetric I-beams", *Engineering Structures*, **34**, 564-571, 2012.

[16] Surla A.S., Kang S.Y. and Park J.S., "Inelastic bukling assessment of monosymmetric I-beams having stepped and non-compact flange sections", *Journal of Constructional Steel Research,* **114**, 325-337, 2015.

[17] Tankova T., Rodrigues F., Leitão C., Martins C., Simões da Silva L., "Lateral-torsional buckling of high strength steel beams: Experimental resistance", *Thin-Walled Structures*, **164**, 107913, 2021.

[18] Yang B., Kang S.B., Xiong G., Nie S., Hu Y. and Wang S., "Experimental and numerical study on lateral-torsional buckling of singly symmetric Q460GJ steel I-shaped beams", *Thin-Walled Structures,* **113**, 205–16, 2017.

[19] Kang S.B., Yang B., Zhang Y., Elchalakani M. and Xiong G., "Global buckling of laterally unrestrained Q460GJ beams with singly symmetric I-sections", *Journal of Constructional Steel Research,* **145**, 341–51, 2018.

[20] Zhao J., Li J. and Sun Y., "Experimental and numerical study on overall buckling behavior of Q460 high-strength steel continuous beams with welded singly symmetric I-section", *Engineering Structures*, **280**, 115678, 2023.

[21] Bradford M.A. and Cuk P.E., "Elastic buckling of tapered monosymmetric I-beams", *J. Struct. Eng*, **114**, 977-996, 1988.

[22] Andrade A. and Camotim D., "Lateral-torsional buckling of singly symmetric tapered beams: theory and applications", *J Eng Mech.,* **131**, 586-597, 2005.

[23] Andrade A., Camotim D. and Dinis P.B., "Lateral-torsional buckling of singly symmetric web-tapered thin-walled I-beams: 1D model vs. shell FEA", *Computers and Structures*, **85**, 1343-1359, 2007.

[24] Cockalingam S.N., Pandurangan V. and Nithyadharan M., "Timoshenko beam formulation for in-plane behavior of tapered monosymmetric I-beams: Analytical solution and exact stiffness matrix", *Thin-Walled Structures*, **162**, 107604, 2021.

[25] Trahair N.S., "Bending and buckling of tapered steel beam structures", *Thin-Walled Structures*, **59**, 229–237, 2014.

[26] Trahair N.S., "Lateral buckling of tapered members", *Engineering Structures*, **151**, 518–526, 2017.

[27] Marques L., Simões da Silva L., Greiner R., Rebelo C. and Taras A., "Development of a consistent design procedure for lateral-torsional buckling of tapered beams", *Journal of Constructional Steel Research*, **89**, 213-235, 2013.

[28] Tankova T., Martins J.P., Marques L., Simões da Silva L., Santiago A. and Craveiro H., "Experimental lateral-torsional buckling behavior of web-tapered steel beams", *Engineering Structures*, **168**, 355-370, 2018.

[29] Lebastard M., *Stability of welded I-section steel members*, PhD Thesis, INSA Rennes, France, 2022.

[30] Tankova T., Simões da Silva L. and Marques L., "Buckling resistance of non-uniform steel members based on stress utilization: general formulation", *Journal of Constructional Steel Research*, **149**, 239-256, 2018.

[31] Tankova T., Marques L., Andrade A., Simões da Silva L., "Development of a consistent methodology for the out-of-plane buckling resistance of prismatic beam-columns", *Journal of Constructional Steel Research*, **128**, 839-852, 2017.

[32] European Committee for Standardization – *EN 1993-1-1:2005. Eurocode 3: Design of steel structures. Part 1-1: General rules and rules for buildings*. Brussels, 2005.

[33] Simões da Silva L., Marques L. and Rebelo C., "Numerical validation of the general method in EC3-1-1: lateral, lateral-torsional and bending and axial force interaction of uniform members", *Journal of Constructional Steel Research*, **66**, 575-590, 2010.

[34] Simões da Silva L., Tankova T., Marques L., Rebelo C. and Taras A., "Safety assessment of EC3 stability design rules for the lateral-torsional buckling of prismatic beams", *Advanced Steel Construction*, **14**(4), 668-693, 2018.

[35] Chen F. and Atsuta T., *Theory of Beam-Columns. Vol. 2: Space behaviour and design*. McGraw-Hill, Inc., 1977.

[36] Wagner H., Torsion and Buckling of Open Sections, NACA Tech. Mem., n. 807, 1936.

[37] Ansys Inc. *Release 22.0 – Documentation for Ansys*. Canonsburg, United States, 2021.

[38] European Convention for Constructional Steelwork – *ECCS. Manual on Stability of Steel Structures*, 2. Ed. Liège, Belgium, 1976.

[39] European Committee for Standardization – *prEN 1993-1-14 - draft. Eurocode 3 – Design of steel structures – Part 1-14: Design assisted by finite element analysis*. Brussels, 2021.